Chinese Journal of Chemical Engineering 40 (2021) 27–35

Contents lists available at ScienceDirect

Chinese Journal of Chemical Engineering

journal homepage: www.elsevier.com/locate/CJChE

Full Length Article

Mass transfer coefficient in the eductor liquid-liquid extraction column

Bahare Esmaeeli, Ahad Ghaemi *, Mansour Shirvani, Mostafa Hosseinzadeh

School of Chemical, Petroleum and Gas Engineering, Iran University of Science & Technology, Narmak, Tehran, Iran

ARTICLE INFO

Article history:
Received 24 July 2020
Received in revised form 17 November 2020
Accepted 1 December 2020
Available online 31 December 2020

Keywords:
Gasoil desalting
Liquid-liquid extraction
Eductor-LLE device
Mass transfer coefficient
Extraction efficiency

ABSTRACT

In this research gasoil desalting was investigated from mass transfer point of view in an eductor liquid–liquid extraction column (eductor-LLE device). Mass transfer characteristics of the eductor-LLE device were evaluated and an empirical correlation was obtained by dimensional analysis of the dispersed phase Sherwood number. The Results showed that the overall mass transfer coefficient of the dispersed phase and extraction efficiency have been increased by increasing Sauter mean diameter (SMD) and decreasing the nozzle diameter from 2 to 1 mm, respectively. The effects of Reynolds number (*Re*), projection ratio (ratio of the distance between venturi throat and nozzle tip to venturi throat diameter, R_{pr}), venturi throat area to nozzle area ratio ($R_{th\text{-}n}$) and two phases flow rates ratio (R_Q) on the mass transfer coefficient (K) were determined. According to the results, K increase with increasing *Re* and R_Q and also with decreasing R_{pr} and $R_{th\text{-}n}$. Semi-empirical models of drop formation, rising and coalescence were compared with our proposed empirical model. It was revealed that the present model provided a relatively good fitting for the mass transfer model of drop coalescence. Moreover, experimental data were in better agreement with calculated data with AARE value of 0.085.

1. Introduction

Desalting of liquid solutions may be done by liquid–liquid extraction (LLE) in which a solute is removed from a liquid by a solvent in two immiscible liquid systems [1]. LLE is a simple separation technique with an appropriate mass transfer rate, used in many industries such as hydro-metallurgy, and chemical industries like oil refining, pharmaceutical also environmental applications [2]. The mixing in the LLE system can be created either with agitation or without agitation [3]. In the case of no agitation device, the mechanism of mixing should be done with some kind of jet flow. Three different regimes may occur when a liquid is injected as a jet flow into another liquid in LLE systems [4]. A dripping regime will be formed at low velocities of flow through the nozzle, while by increasing velocity the dripping regime converts to jetting flow. The length of jet flow decreases with increasing velocity leading to appearance of the atomization regime. Nozzle and orifice mixers are the most conventional industrial jet mixers with acceptable performances for crude oil desalting [1].

Impinging-jets accelerate the mixing of two liquid phases compared to the conventional extractor, leading to increased mass transfer coefficient and reduced volume of the device for a required mass transfer rate [5]. In this device, it was proved that the addition of NaCl to the system of toluene/acetone/water has an improving effect on the extraction efficiency and mass transfer coefficient [6]. Ejectors as a jet type system are also used widely in chemical process industries [7]. It has been used in an LLE device and provides an appropriate mass transfer rate [8]. Limited studies on the use of ejectors in the LLE process have been reported. Suresh *et al.* [9] have used the countercurrent separation process of uranium and thorium with a multi-stage ejector using the LLE device, i.e. mixer-settler and evaluated its performance. Eductor is a type of ejector for mixing two liquids that can be used as a mixer in the LLE process [10]. In comparison to some other LLE devices such as rotating disc contactors which have moving parts, sealing problem as well as corrosion do not exist in eductor-LLE devices [11]. In an eductor-LLE device, a venturi is placed in front of the nozzle; The main parts of the device are shown as the venturi and the nozzle in Fig. 1. The dispersed phase flow enters venturi after the nozzle and pulls the continuous phase flow into venturi [12]. The dispersed phase flow through nozzle tip enters the venturi and the continuous phase flow around the venturi is sucked into the venturi. The mixing of these two phases is maximized at the venturi throat and exits through the venturi as a mixture. The exiting flow of dispersed phase from the venturi is sucked back into the venturi along with the continuous phase flow. In recent studies, the hydrodynamic performance of eductor-LLE devices was partly

* Corresponding author. Fax: +98 2177240495.
E-mail address: aghaemi@iust.ac.ir (A. Ghaemi).

https://doi.org/10.1016/j.cjche.2020.12.017
1004-9541/

verified using computational fluid dynamics (CFD), as well as the modeling of Sauter mean diameter (SMD) [13,14].

The mass transfer coefficient between the two phases in LLE systems is an important parameter for determining the performance of the extractor [15]. Rajagopalan *et al.* [16], studied an air-pulsed ejector mixer settler in nuclear industries and reported a high mass transfer performance. Mass transfer between jet flow and its surrounding flow is discussed by Sawistowski in jet breakup system [17]. It was claimed that mass transfer inside the jet increases in an opposite trend compared to mass transfer outside the jet. Acharje *et al.* [18] studied water/*n*-butanol and water/methyl-ethyl-ketone systems in an ejector device and presented a correlation to calculate the mass transfer coefficient. Suresh *et al.* [19] studied on performance of a counter-current ejector mixer-settler LLE device for uranium–thorium separation and reported higher extraction efficiency. The effect of mass transfer on jet breakup in liquid laminar jet in gas phase, and liquid jets in liquid phase are studied by Burkholder & Berg [20]. Kimura & Miyauchi [21] determined mass transfer rate in liquid–liquid laminar jet with diffusion equation by measuring the approximate interfacial velocity using photographic technique. Cheng *et al.*[22] investigated the characteristics and mechanism of melt jet breakup in water and reported that Rayleigh-Plateau instability had the dominant effect on the melt jet column breakup in water. Saien *et al.* [23] investigated mass transfer enhancement in a jet LLE device with dimensionless modeling. Various LLE devices with jet mixing were studied by Tamir, reporting that the jet streams can raise the mass transfer coefficient, significantly [24]. Numerous correlations for mass transfer coefficient of different extraction columns have been obtained using different chemical systems: single drops [25,26], rotating disc contactors (RDC) [27], perforated rotating disc contactor (PRDC) [28,29], Kühni [30], pulsed perforated-plate [31] and multistage column [32].

The conventional LLE devices have some disadvantages such as corrosion and sealing problems and so much space requirements [11]. Due to the presence of venturi against nozzle flow, the eductor has advantages over jet systems, which can be referred to as high efficiency and more mixing. Therefore, the eductor LLE device provides some advantages such as less sealing and corrosion problems, low contact time, no requirement for moving parts, provision of high overall mass transfer coefficients and reduced contactor volume [14]. But, the mass transfer characteristic of an eductor-LLE device is not yet investigated. In the present study, mass transfer characteristics of the eductor-LLE device for separation of NaCl from gasoil by water are evaluated, experimentally and theoretically.

2. Experimental

2.1. Eductor extractor

A schematic of the experimental set up is shown in Fig. 2. It consists of the main LLE column with the peripheral equipment involving: pumps, valves, three flowmeters, feed and product storage tanks. The continuous phase enters the column from the top through a conic duct, while the dispersed phase is pumped through the nozzle at the bottom. Two-phase separation occurs at the column top and the height of the interface position is manually maintained by adjusting the output of the dispersed phase. Two of the flowmeters are used for these two phases input flow rates, while the third one is used for the output of the continuous phase flow rate. The flow of dispersed phase from the nozzle which enters the eductor, helps in sucking some amount of continuous phase into the venturi, so there are distributions and mixing inside the venturi throat.

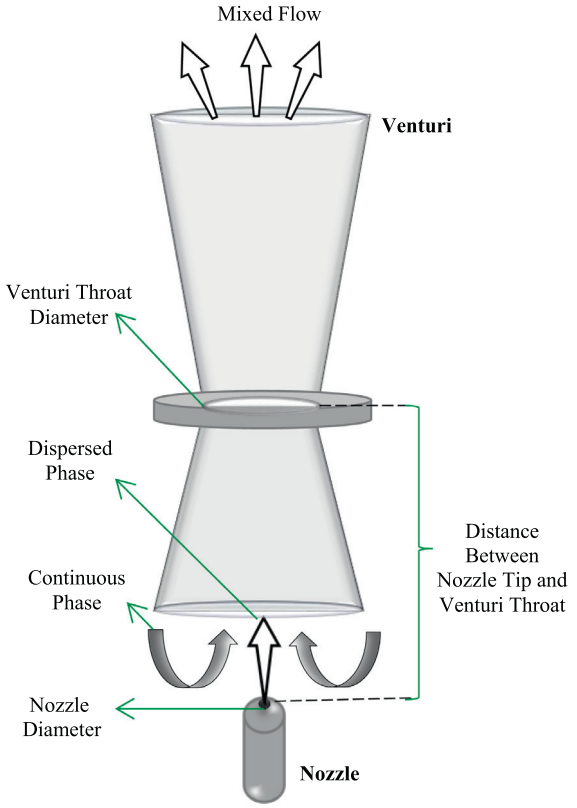

Fig. 1. Schematic of eductor.

Table 1 gives the geometrical parameters of the device used in the experiments. Collected data in this table were evaluated by the CFD results and were used to design the eductor-LLE device [13]. The number of experiments required in this work was obtained using the CCD (central composite design) method for investigating the effects of nozzle diameter (D_n), venturi throat diameter (D_{th}), nozzle tip distance from venturi throat ($L_{th\text{-}n}$), jet velocity (V_j) and two phases flow rates ratio (R_Q) on the overall mass transfer coefficient of the dispersed phase (commonly abbreviated as K).

2.2. Water-gasoil desalting system

A Purified gasoil (from sulfur components) supplied by Kimia Azma Company, Tehran, Iran was saturated with NaCl to be used as a dispersed phase. Deionized water was selected as a continuous phase to remove NaCl from gasoil in a countercurrent system. The reason for performing the experiments with saturated gasoil was to prevent interference of any trivial impurities during mass transfer between the two phases. The physical properties of the used materials in the current LLE system, including their viscosity, density and specific interfacial area were measured by Kimia Azma Company, Tehran, Iran.

One of the acceptable relationships for measuring molecular diffusivities of NaCl into gasoil and deionized water (D), as another physical property of the chemical system, is the Wilke-Chang equation [33].

$$D = \left(7.4 \times 10^{-8}\right) M^{\frac{1}{2}} T / \mu V_A^{0.6} \quad (1)$$

where M, T, and V_A are the molecular weight of solvent, temperature and molal volume of solute at normal boiling point. These physical properties are presented in Table 2. In this research, all experiments have been performed at ambient temperature.

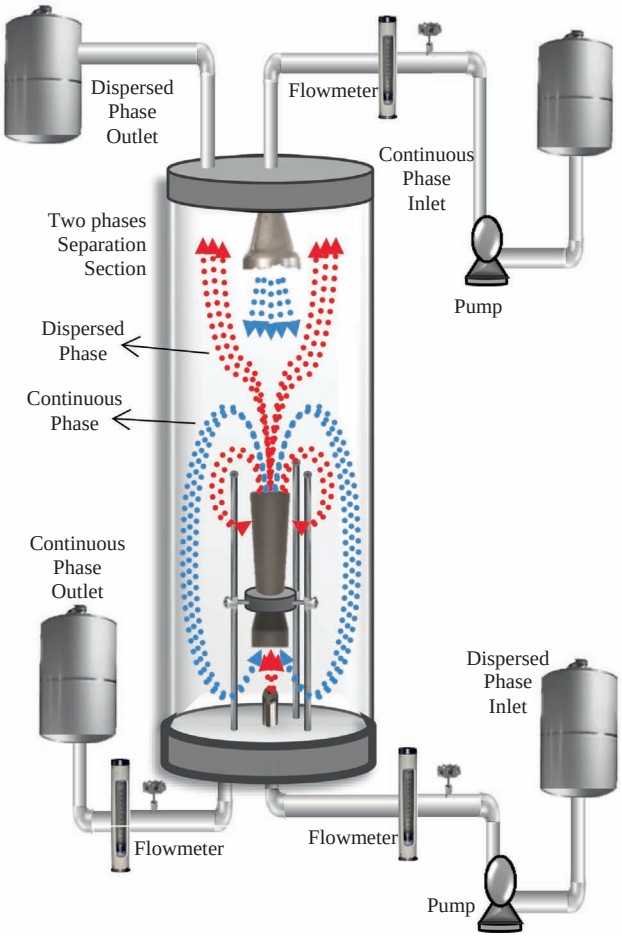

Fig. 2. Experimental set-up.

Table 1
Geometrical parameters of eductor-LLE device

Parameter	Value
Venturi divergence angle (output)	7°
Venturi convergence angle (input)	45°
Overall length of venturi	0.10 m
Venturi throat diameters (D_{th})	0.01, 0.02 and 0.03 m
Distance between venturi throat and nozzle ($L_{th\text{-}n}$)	0.01, 0.02 and 0.03 m
Nozzle diameters (D_n)	0.001, 0.002 and 0.003 m

Table 2
Physical properties of the gasoil/NaCl/water system at 20 °C

Physical Property	Continuous	Dispersed
ρ/kg·m^{-3}	995.7	734
μ/Pa·s	1,075,000	500,000
σ/N·m^{-1}	0.0198	
$\Delta\rho$/kg·m^{-3}	261.7	
D_c/m^2·s^{-1}	$10^{-9} \times 1.36$	
D_d/m^2·s^{-1}	8.03×10^{-9}	

The method of electrical conductivity (EC) is one of the most accurate methods for measuring the salt concentration in water products [34]. The concentration of NaCl in the continuous phase was analyzed as total dissolved solid (TDS), *via* a TDS tester, model 6032 of the Taiwanese company, EZDO, with a replaceable electrode. Fig. 3 shows the calibration curve prepared for determining

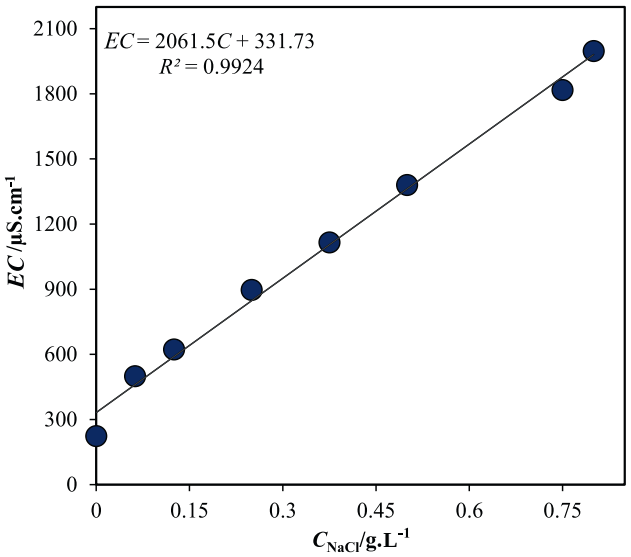

Fig. 3. Electrical conductivity (*EC*) of concentration of NaCl in water.

the EC of various concentrations of NaCl in deionized water. This liner curve fitting of measured data yields the R^2 value of 0.9924 which represents the goodness of fitting as a statistic variable. So this curve is considered acceptable for use in concentration measurements.

The following relation was derived to achieve the equilibrium concentration of NaCl in the dispersed phase ($C^*_{d,out}$).

$$C^*_{d,out} = 1.3396 C^{1.0418}_{c,out} \quad (2)$$

where $C_{c,out}$ is the concentration of NaCl in the continuous phase corresponding to $C^*_{d,out}$. By determination of the flow rates of both phases, $C_{c,out}$ can be obtained using the mass balance method (see a schematic diagram of this process in Fig. 4). Thereafter $C^*_{d,out}$ can be calculated by Eq. (2). In this Equation, in order to obtain an equilibrium curve, different concentrations of water and salt were first prepared and mixed in equal proportions with gasoil. After complete mixing and equilibrium of the two phases, the continuous phase was separated and the salt concentration was measured. By means of mass balance, the salt concentration in the gasoil was obtained. Also by help of about more than 15 equilibrium points in the study concentration range, the above relationship was obtained with a higher accuracy. The value of R^2 for the above relation is 0.9597.

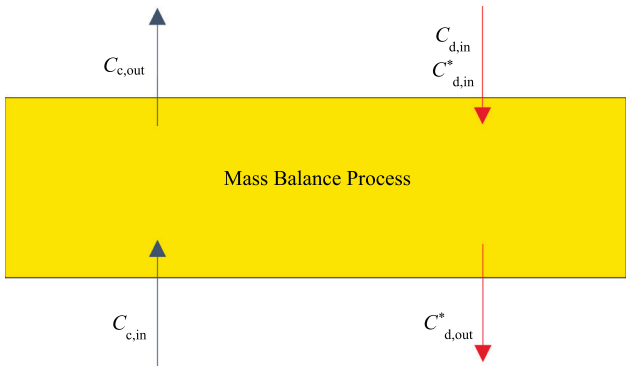

Fig. 4. Schematic diagram of the mass balance process.

2.3. Procedure and analysis

2.3.1. Extraction efficiency and mass transfer coefficient

In this work the mass transfer direction is from dispersed phase to continuous phase (d→c), then the extraction efficiency can be represented as:

$$E = (C_{d,in} - C_{d,out})/(C_{d,in} - C^*_{d,out}) \quad (3)$$

where $C_{d,in}$ and $C_{d,out}$ are inlet and outlet concentrations of NaCl in the dispersed phase, respectively. $C^*_{d,out}$ is the equilibrium concentration of NaCl in the outlet dispersed phases, corresponding to the outlet NaCl concentration in the continuous phase. The solubility of the solute in the continuous phase is much higher than its solubility in the dispersed phase. Hence, the mass transfer resistance of continuous phase is negligible as the fact that continuous input phase is free of solute. Therefore, all resistance to mass transfer is in the dispersed phase. According to experimental data, the mass transfer coefficient ($K_{calc.}$) of the dispersed phase can be calculated by Eq. (4).

$$R = Q_d(C_{d,in} - C_{d,out}) = K_{calc.} a v \Delta C_m \quad (4)$$

where R, Q_d, a, and v are mass transfer rate (or extraction rate), the volumetric flow rate of the dispersed phase, specific interfacial area and the effective volume column, respectively. Besides, ΔC_m is a mean concentration driving force that is a common practice to use logarithmic mean concentration deriving force, ΔC_{ln}, instead of ΔC_m in Eq. (4) since the mixing condition of the two phases is not known. ΔC_{ln} can be calculated using the following equation [35].

$$\Delta C_{ln} = \frac{(C^*_{d,out} - C_{d,out}) - (C_{d,in} - C^*_{d,in})}{\mathrm{In}((C^*_{d,out} - C_{d,out})/(C_{d,in} - C^*_{d,in}))} \quad (5)$$

where $C^*_{d,in}$ is the equilibrium concentration of NaCl in the inlet dispersed phase, corresponding to the inlet NaCl concentration in the continuous phase. In order to achieve the mass transfer coefficient as shown in Eq. (4), the specific interfacial area is determined by the following equation (Eq (6)) [36].

$$a = 6\varphi/D_{32} \quad (6)$$

According to the definition of Eq. (6) essential parameters for calculating specific interfacial area are: (a) Sauter mean diameter (SMD), (b) the holdup.

(a) Normally, in the extraction columns, the drops have wild size ranges but Sauter is proposed to represent a single value for the diameter of different-size drops. In each experiment, the image processing method which is a method for analyzing video films, was used to measure the velocity of drops rising. The selected area for capturing videos is the venturi output (the upper part of the venturi). Moreover, photos were also taken to measure the diameter of drops. A suitable camera with 60 frames per second is used which the quality of photo and video were 4160 × 3120 and 1920 × 1080 pixels, respectively. The following equation can be used to calculate SMD in the eductor-LLE device.

$$D_{32} = \frac{\sum_{i=1}^{N} N_i d_i^3}{\sum_{i=1}^{N} N_i d_i^2} \quad (7)$$

where N_i and d_i are the number and diameter of the drops, respectively.

(b) The holdup is the ratio of the volume fraction of the dispersed phase to the total volume of liquids at the interface between the phases appearing above the column. Holdup measurement was performed by simultaneously stopping the flow of continuous and dispersed phases and allowing complete separation of the phases by changing the interphase height position at the top of the column. In this way, the total amount of dispersed phase holdup can be obtained by giving enough time to raise all the drops (drops coalescence of dispersed phase).

2.3.2. Modeling

Regarding the complexity of mass transfer in LLE devices, the essential equations for mass transfer coefficient are seldom available. Instead, empirical methods are almost conducted to obtain a related dimensionless correlation [37]. In LLE systems the operating variables should be varied systematically to determine their influence on Sherwood number of the dispersed phase (Sh_d). The general format of Sh_d correlation is a function of Reynolds number and Schmidt number (Sc_d).

$$Sh_d = f(Re, Sc_d) \quad (8)$$

where

$$Sc_d = \mu_d/\rho_d D_d \quad (9)$$

The empirical correlation of the Sh_d is based on the operating variables (D_n, D_{th}, and $L_{th\text{-}n}$) and physical properties (Q_d, Q_c, and V_j) of the system. Therefore, the Sh_d depends on the dimensionless parameters. According to Buckingham pi theorem for dimensional analysis the Sh_d can be given by Eq. (11):

$$Sh_d = \frac{K_{exp} D_{32}}{D_c} = C_0 Re^{C_2} R_{th-n}^{C_3} R_{pr}^{C_4} R_Q^{C_5}, \quad C_0 = c_0 Sc^{C_1} \quad (11)$$

Constant C_0, *i.e.* c_0 ScC_1 as well as C_2, C_3, C_4, and C_5 exponents should be obtained by the least square fitting method. The ranges of the dimensionless parameters, *i.e.* Reynolds number (Re), venturi throat area to nozzle area ratio ($R_{th\text{-}n}$), the projection ratio (ratio of the distance between venturi throat and nozzle tip to venturi throat diameter, R_{pr}) and two phases flow rates ratio (R_Q), in Table 3 are shown. The equations of these dimensionless parameters are as follows.

$$Re = \rho_d V_j D_n/\mu_d \quad (12)$$

$$R_{th-n} = A_{th}/A_n = {D_{th}}^2/{D_n}^2 \quad (13)$$

$$R_{Pr} = L_{th-n}/D_{th} \quad (14)$$

$$R_Q = Q_d/Q_c \quad (15)$$

2.3.3. Mass transfer during drop formation, rising and coalescence stages

Dispersed phase mass transfer is divided into three stages, including: drop formation stage, drop falling or rising stage and drop coalescence stage. Skelland and Huang [38] have shown that the mass transfer coefficient of these three stages under the non-jetting regime can be extended to the jetting region with success. The semi-empirical equations of mass transfer coefficient for drop formation and coalescence were reported and also provided an equation for the rising of oscillating drops. These above equations are presented below:

(1) Drop formation correlation (Eq. (16)) was proposed by Skelland and Minhas [39]:

Table 3
Ranges of dimensionless parameters in the empirical correlation of the Sh_d

Title	Description
System	Gasoil/NaCl/water
Re	934–3885
$R_{th\text{-}n}$	11.11–400
R_{pr}	0.33–2
R_Q	1.3–3

$$K_{\text{drop formation}} = 0.0432\left(\frac{D_{32}}{t_f}\right)\left(\frac{V_d^2}{D_{32}g}\right)^{0.089}\left(\frac{{D_{32}}^2}{t_f D_d}\right)^{-0.334}\left(\frac{\mu_d}{\sqrt{\rho_d D_{32}\sigma}}\right)^{-0.601} \quad (16)$$

where t_f, V_d, and g are the time of drop formation, the velocity of rising drops and acceleration due to gravity, respectively. As previously observed, the physical properties of the gasoil/NaCl/water system are presented in Table 2 and the image processing method was used to calculate the rising drop velocity. The formation time of the drop is also calculated as the following equation.

$$t_f = \pi {D_{32}}^3 / 6Q_d \quad (17)$$

(2) Drop rising (oscillating drops) correlation (Eq. (18)) was proposed by Skelland and Wellek [40]:

$$K_{\text{drop rising}} = 0.32\left(\frac{D_d}{D_{32}}\right)\left(\frac{4tD_d}{{D_{32}}^2}\right)^{-0.14}\left(\frac{D_{32}V_S\rho_c}{\mu_c}\right)^{0.68}\left(\frac{{\rho_c}^2\sigma^3}{g\Delta\rho{\mu_c}^4}\right)^{0.10} \quad (18)$$

where t is the time of rising drops and V_S denote slip velocity between continuous and dispersed phases in the column which may be calculated as:

$$t = \varphi v / Q_d \quad (19)$$

$$V_S = V_d/\varphi + V_c/(1-\varphi) \quad (20)$$

(3) Drop coalescence correlation (Eq. (21)) was proposed by Skelland and Minhas [39]:

$$K_{\text{drop coalescence}} = 0.173\left(\frac{D_{32}}{t_f}\right)\left(\frac{\mu_d}{\rho_d D_d}\right)^{-1.115}\left(\frac{g\Delta\rho{D_{32}}^2}{\sigma}\right)^{1.302}\left(\frac{V_S^2 t_f}{D_d}\right)^{0.148} \quad (21)$$

A comparison can be made using the average absolute value of relative error, AARE, between the experimental and calculated data. Moreover, AARE is also used to evaluate the accuracy of the proposed correlation (Eq. (22)).

$$\text{AARE} = \frac{1}{N}\sum_i^N \left|\frac{K_i^{\text{calc.}} - K_i^{\text{exp.}}}{K_i^{\text{exp}}}\right| \quad (22)$$

where N and K are the number of experimental data and mass transfer coefficient, respectively.

3. Results and Discussion

In the current study, the mixing within the eductor-LLE device has been improved with the existence of a venturi in front of the nozzle at specific Reynolds numbers. The experimental data were obtained from 36 runs. On this basis, the effects of four variables Re, $R_{\text{th-n}}$, R_{pr}, and R_Q as well as some other parameters will be illustrated on the mass transfer coefficient in the next sessions.

3.1. Effect of SMD

As shown in Fig. 5, with increasing Sauter mean diameter (SMD) the mass transfer coefficient increases. The figure is plotted for three different nozzle diameters. As illustrated above, it can be seen that the size of drops increases with increasing nozzle diameter, because of enhancement in circulation inside the drops. This finally leads to an increased mass transfer coefficient [41,42]. Therefore, in an overall conclusion, the mass transfer coefficient can improve by increasing the nozzle diameter. A notable conclusion here is that with an increase in nozzle diameter the slope of mass transfer coefficient increases sharply. This can be explained in view that the internal circulation in the gasoil drops changes dramatically by variation of drop size. when the size of drop is large, the interfacial phenomena occur faster [43]. Therefore, phenomena of interfacial instability can facilitate mass transfer and increase the mass transfer coefficient with a sharp slope at 3 nozzle diameter.

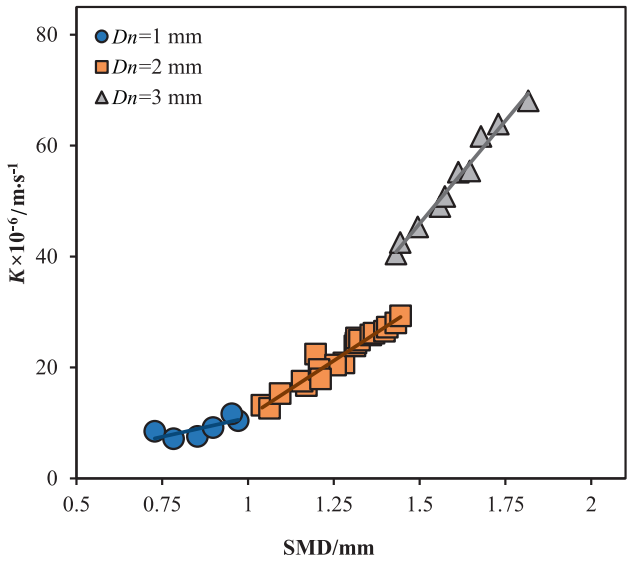

Fig. 5. Effect of SMD on mass transfer coefficient for different nozzle diameters.

3.2. Extraction efficiency

The extraction efficiency, according to Eq. (3), was obtained in the range of 37.5%–93.7%. Fig. 6 shows the effect of nozzle diameter on extraction efficiency at various Reynolds numbers. The results show minimum extraction efficiency at nozzle diameter around 2 mm, along with a slight increase in efficiency with increasing Reynolds number. This argument can be presented in view that higher efficiency at lower nozzle diameters is the result of increasing contact surface area of mass transfer between the two phases, due to a reduction in drop size. While increasing the nozzle diameter from 2 mm to 3 mm in a constant Reynolds number,

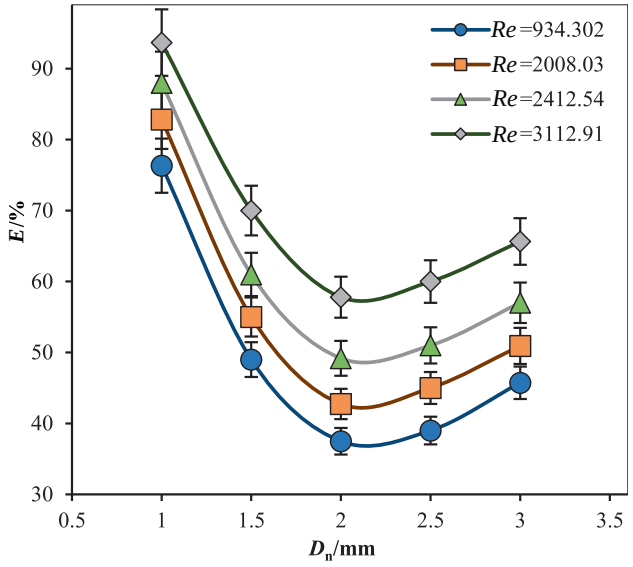

Fig. 6. Effect of nozzle diameter on extraction efficiency for different Reynolds numbers.

increases the extraction efficiency with a slight slope. As previously seen in Fig. 5, the nozzle diameter is the dominant and influential parameter which the mass transfer coefficient increases with increasing D_n [44]. Thus, due to the increase in drops size and internal circulation in the drops, the extraction efficiency increases. However, a decrease in D_n less than 2 mm increases extraction efficiency with a sharp slope which means that the large contact surface area of the drop with the surrounding liquid has a greater effect on increase the extraction efficiency. Furthermore, increasing Reynolds number at a constant nozzle diameter (i.e. the increasing mixing and turbulence with an increase in jet velocity) increases the extraction efficiency.

3.3. Effect of Reynolds number on the mass transfer coefficient in the eductor LLE-device

Fig. 7. shows the graph of mass transfer coefficient against Reynolds number for difference venturi throat area to nozzle area ratios ($R_{th\text{-}n}$). The range of Reynolds number, as a main effective parameter, was calculated between 934 and 3885 so internal circulations can be seen in all drops. As expected, the figure shows that the Reynolds number has a positive effect on the mass transfer coefficient for all values of $R_{th\text{-}n}$. Indeed, the higher Reynolds number results in higher turbulence and subsequently increases the mass transfer coefficient [45].

3.4. Effects of dimensionless parameters on the mass transfer coefficient in the eductor LLE-device

3.4.1. Effect of throat area to nozzle area ratio

Fig. 8a shows that the mass transfer coefficient increases with decreasing venturi throat area to nozzle area ratio ($R_{th\text{-}n}$). Since $R_{th\text{-}n}$ is the ratio of venturi throat diameter squared (D_{th}^2) to nozzle diameter squared (D_n^2), therefore $R_{th\text{-}n}$ can reduced in two cases: decrease in D_{th} and increase in D_n. In the former case, the mixing process occurs in less space leads to an increase in the mass transfer coefficient. In the latter case, an increase in D_n results in larger drops formation and the liquid motion inside these large drops increases the mass transfer coefficient as discussed before. It should also be noted that the high jet velocity converts drop to smaller drops and causes the emulsion formation. Also, there are no internal circulations in the too-small formed drops [46]. For these reasons, the high mass transfer cannot be achieved in low nozzle diameters. As mentioned above, the increase in Reynolds number

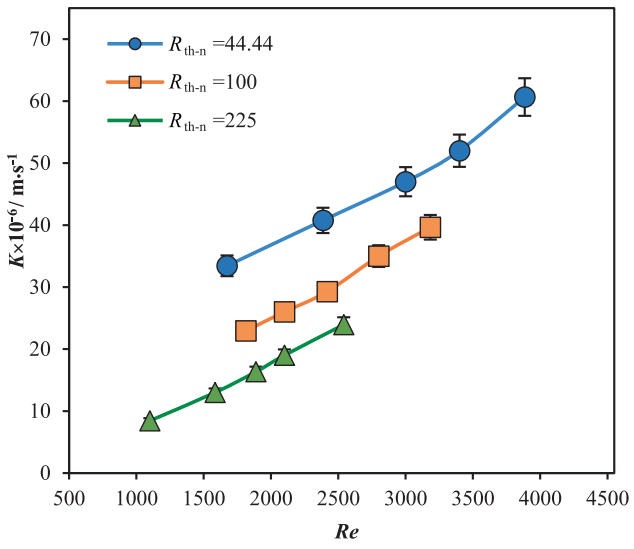

Fig. 7. Effect of Reynolds number on mass transfer coefficient for different ratios of venturi throat area to nozzle area.

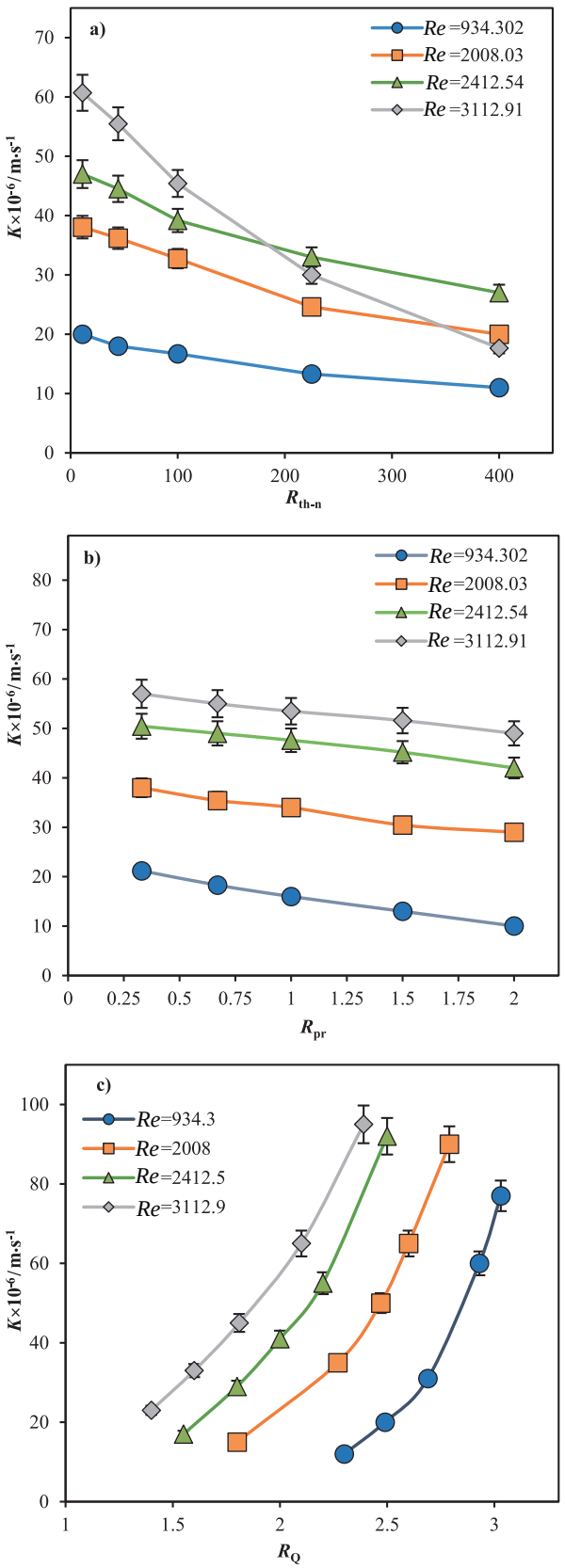

Fig. 8. Effect of (a) venturi throat area to nozzle area ratio, (b) projection ratio, and (c) two phases flow rates ratio on mass transfer coefficient for different Reynolds numbers.

has an increasing effect on the mass transfer coefficient. Thus we can see a sharp increase in the mass transfer coefficient slope at the highest Reynolds number value.

3.4.2. Effect of projection ratio

Fig. 8b shows that contrary to the Reynolds number, the projection ratio (R_{pr}) reveals a decreasing effect on the mass transfer coefficient. This can be argued that with increasing R_{pr} the mixing efficiency decreases because the distance of nozzle from venturi throat ($L_{th\text{-}n}$) increases [13]. Thus, at lower projection ratio values the turbulence and mixing become better and as a result, the mass transfer coefficient improves with a decrease in R_{pr}. Because jet energy in the entrance of the venturi throat is higher in the lower $L_{th\text{-}n}$ and more mixing intensity occurs in the venturi. It should be stressed that the lower $L_{th\text{-}n}$ leads to faster jet breakup and drop formation. Hence with increasing the number of drops resulting from high-energy jet breakup and an increase in two-phase contact surface area with a high level of turbulence improve the mass transfer coefficient. In other words, in the low nozzle to venturi throat distances or high-energy jet, higher suction rates are attainable so better mixing is done. This behavior is because of the higher shear forces that apply on phases and increase the turbulence of the bulk.

3.4.3. Effect of two phases flow rate ratio

Fig. 8c reveals that the mass transfer coefficient increases sharply with increasing two phases flow rates ratio (ratio of dispersed phase to continuous phase flow rates, R_Q) at different Reynolds numbers. By decreasing R_Q or in other words, an increase in continuous phase flow rate (Q_c) that inserts from the top of the column in the opposite direction of the venturi outlet, the mixing and subsequently mass transfer coefficient decrease. Because an increase in Q_c leads to enhancement in pressure drop and finally reduces the mixing. Moreover, with increasing Q_c, the countercurrent mixing streams are decreased despite the reduction in jet and drops rising velocity. When the intensity of the Q_c is low, the jet flow has more opportunities for better mixing and mass transfer. An increase in mixing intensity has a direct effect on the mass transfer rate and improves the mass transfer coefficient. On the other hand by increasing R_Q or increasing dispersed phase flow rate (Q_d) the mass transfer coefficient increases. Due to enhancement in the interfacial mass transfer area and the mechanism of surface-renewal generated by eddies. Besides, the rapid dispersed phase drop rising in the counter flow of continuous phase in the column causes faster drop coalescence and improved internal mixing which in turn improves the mass transfer coefficient.

3.5. Mass transfer coefficient correlation

The empirical correlation (Eq. (23)) is expanded in order to obtain the experimental mass transfer coefficient according to Eq. (24).

$$Sh_d = 14.676 Re^{0.856} R_{th-n}^{-0.403} R_{pr}^{-0.448} R_Q^{0.348} \quad (23)$$

$$K_{exp} = 14.676 \left(\frac{D_c}{D_{32}}\right) \left(\frac{\rho_d V_j D_n}{\mu_d}\right)^{0.856} \left(\frac{D_{th}^2}{D_n^2}\right)^{-0.403} \left(\frac{L_{th-n}}{D_{th}}\right)^{-0.448} \left(\frac{Q_d}{Q_c}\right)^{0.348} \quad (24)$$

The above empirical correlation reveals that the Reynolds number has more effective than the other three dimensionless parameters, while the $R_{th\text{-}n}$ and R_{pr} have effects of decreasing. Fig. 9 shows that, experimental values obtained from Eq. (24) were compared with calculated values from Eq. (4). There is a very good agreement between experimental mass transfer coefficients ($K_{exp.}$) and calculated mass transfer coefficients ($K_{calc.}$). The regression coefficient (R^2) value is 97.66%.

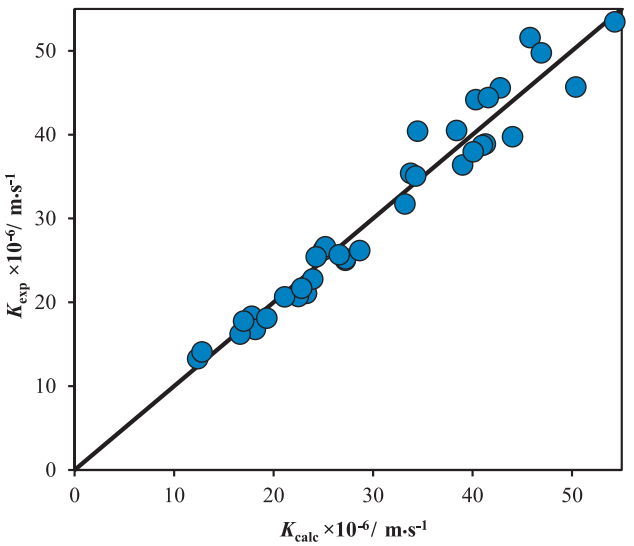

Fig. 9. Comparison of experimental values of mass transfer coefficient with calculated values from model.

3.6. Investigation of mass transfer coefficient semi-empirical correlation

Mass transfer coefficient correlation of the eductor-LLE device was compared with single drop semi-empirical correlations during drop formation, rising and coalescence. The results are discussed in Fig. 10. These results exhibit that these semi-empirical correlations in the single drop system are not suitable for prediction $K_{exp.}$ in this device. As can be seen in Fig. 10, the derived model presents better fitness than other discussed models (Eqs. (16), (18) and (21)). Most researchers have reported that the mass transfer coefficient during drop coalescence is negligible [47–50]. However, the results show that in the eductor-LLE device, the highest mass transfer fraction

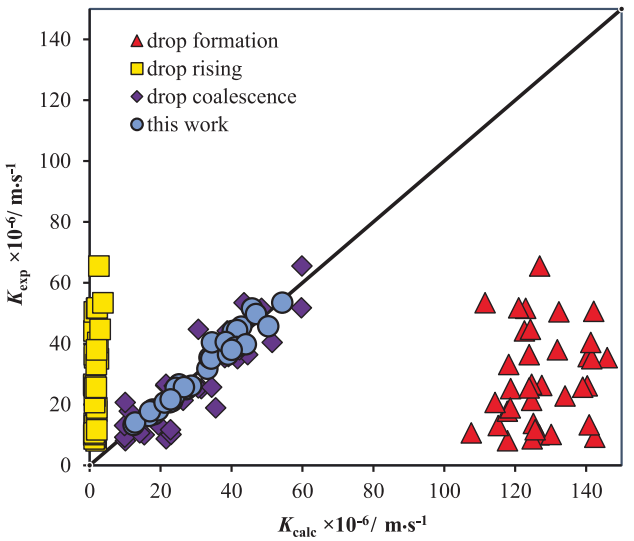

Fig. 10. Comparison of experimental data with calculated data during drop formation, rising and coalescence.

Table 4
The AARE values of obtained $K_{exp.}$ compared to $K_{drop\ formation}$, $K_{drop\ rising}$ and $K_{drop\ coalescence}$

Condition	Mass Transfer Coefficient Model	Values of AARE
Drop formation	$K_{drop\ formation}$	16.083
Drop rising (oscillating drops)	$K_{drop\ rising}$	2.569
Drop coalescence	$K_{drop\ coalescence}$	1.208
This work	$K_{exp.}$	0.085

has occurred during drop coalescence. Indeed, the existence of venturi improves the mixing process and causes the formation of small drops due to jet break-up phenomena at venturi throat in a short time. The small rising drops coalesce with each other after exiting venturi immediately. Therefore, the proposed model is in better agreement with the semi-empirical correlation for drop coalescence. Also, a previous study elucidated that faster reduction of the solute concentration and mass transfer direction from dispersed phase to continuous phase (d→c) lead to a reduction in coalescence time [51]. Since the presence of venturi accelerates the removal of the NaCl from the gasoil (d→c) coalescence occurs in a short time. This can be another reason for the good conformity of our model to the drop coalescence model. According to Table 4, the AARE values of the semi-empirical models are 1.208, 2.569 and 16.083. These errors indicate that single drop relationships are not very accurate for the present work. The AARE of $K_{exp.}$ from the empirical model is in good agreement with the experimental data that this AARE value is 0.085. It can be concluded that the proposed correlation in this study is more suitable than the other semi-empirical correlations.

4. Conclusions

An experimental study was conducted to evaluate the mass transfer performance for the gasoil desalting system in the eductor-LLE device. The effects of dimensionless parameters specific to the present device on mass transfer improvement were investigated. The empirical correlation is proposed in order to predict Sherwood number of dispersed phase as a function of Re, R_{pr}, $R_{th\text{-}n}$ and R_Q. Reynolds number is the most effective dimensionless parameter among the other one with an exponent of 0.856. The results indicate that the high Re number has an important role on mass transfer coefficient and extraction efficiency. However, the highest mass transfer coefficient and extraction efficiency occur in maximum and minimum (1 mm and 3 mm) nozzle diameter, respectively. Also, it should be noted that the mass transfer coefficient increases with increasing SMD results of increasing turbulence and mixing. The semi-empirical correlations, *i.e.* models of drop formation, rising and coalescence are not accurate to determine the mass transfer coefficient. Contrary to some previse studies the attained mass transfer coefficient model is better fitted to the mass transfer coefficient model during drop coalescence. Although, experimental values are in better agreement with calculated values of the eductor-LLE device. However, AARE value for the present model was calculated about 0.085 that is less than the AARE value of the drop coalescence model. Therefore, the presented model in the current study is appropriate for the estimation of the mass transfer coefficient in the gasoil desalting system.

Declaration of Competing Interest

The authors declare that they have no known competing financial interests or personal relationships that could have appeared to influence the work reported in this paper.

Nomenclature

A_n	area of nozzle, m^2
A_{th}	area of venturi throat, m^2
a	specific interfacial area, $m^2 \cdot m^{-3}$
C	concentration of nacl, $kg \cdot m^{-3}$
$C_{0,1,\ 2,\ \ldots}$	model parameters
D	molecular diffusivity, $m^2 \cdot s^{-1}$
D_n	nozzle diameter, m
D_{th}	venturi throat diameter, m
D_{32}	Sauter mean diameter, m
d_i	drops diameter, m
E	extraction efficiency
EC	electrical conductivity, $s \cdot m^{-1}$
g	acceleration due to gravity, $m \cdot s^{-2}$
K	overall mass transfer coefficient of the dispersed phase, $m \cdot s^{-1}$
$L_{th\text{-}n}$	distance between venturi throat and nozzle tip, m
M	molecular weight of solvent
N	number of drops
Q	flow rate, $m^3 \cdot s^{-1}$
R	mass transfer rate, $g \cdot s^{-1}$
Re	Reynolds number
$R_{th\text{-}n}$	venturi throat area to nozzle area ratio
R_{pr}	projection ratio
R_Q	two-phases flow rates ratio
Sc_d	schmidt number
Sh_d	sherwood number of the dispersed phase
T	temperature, °C
t	time of drop rising, s
t_f	time of drop formation, s
V_A	molal volume of solute at normal boiling point
V_c	velocity of the continuous phase, $m \cdot s^{-1}$
V_d	velocity of rising drops, $m \cdot s^{-1}$
V_j	jet velocity, $m \cdot s^{-1}$
V_S	slip velocity, $m \cdot s^{-1}$
v	effective volume column of the eductor-lle device, m^3
μ	viscosity, Pa·s
ρ	density, $kg \cdot m^{-3}$
$\Delta\rho$	density difference between phases, $kg \cdot m^{-3}$
σ	interfacial tension, $N \cdot m^{-1}$
φ	holdup of the dispersed phase

Subscripts

c	continuous phase
calc.	calculation
d	dispersed phase
exp.	experimental
in	inlet
out	outlet

Superscripts

*	equilibrium value

References

[1] R.E. Treybal, Liquid Extraction, in: f. edition (Ed.) Mcgraw-Hill Book Company Inc, New York, 1951.
[2] V.S. Kislik, Solvent Extraction: Classical and Novel Approaches, Elsevier, 2011.
[3] T.C. Lo, M.H. Baird, C. Hanson, Handbook of Solvent Extraction, Wiley, New York, 1983.
[4] R. Clift, J. Grace, M. Weber, Bubbles, Drops and Particles, Academic Press, New York, 1978.
[5] A.M. Dehkordi, Application of a novel-opposed-jets contacting device in liquid-liquid extraction, *Chem. Eng. Process* 41 (3) (2002) 251–258.
[6] J. Saien, S. Asadabadi, Salting-out effect of NaCl on the rate of mass transfer of liquid-liquid extraction in a two impinging-jets contacting device, *J. Taiwan Inst. Chem. Eng.* 41 (3) (2010) 295–301.
[7] D.-W. Sun, I.W. Eames, Recent developments in the design theories and applications of ejectors-A review, *J. Ins. Energy* (1995) 65–79.

[8] R.L. Yadav, A.W. Patwardhan, Design aspects of ejectors: Effects of suction chamber geometry, *Chem. Eng. Sci.* 63 (15) (2008) 3886–3897.
[9] A. Suresh, T. Srinivasan, P. Vasudeva Rao, C. Rajagopalan, S. Koganti, U/Th Separation by counter-current liquid-liquid extraction with tri-sec butyl phosphate by using an ejector mixer-settler, *Sep. Pur. Technol.* 39 (10) (2005) 2477–2496.
[10] Ludwig E.E., Applied process design for chemical and petrochemical plants, Gulf Publishing Co., Houston, 1984.
[11] A. Sahu, A.B. Vir, L.S. Molleti, S. Ramji, S. Pushpavanam, Comparison of liquid-liquid extraction in batch systems and micro-channels, *Chem. Eng. Process* 104 (2016) 190–200.
[12] M. Moresi, G. Bartolo Gianturco, E. Sebastiani, The ejector-loop fermenter: description and performance of the apparatus, *Biotechnol. Bioeng.* 25 (12) (1983) 2889–2904.
[13] M. Hosseinzadeh, A. Ghaemi, M. Shirvani, Hydrodynamic performance evaluation of a novel eductor liquid-liquid extractor using CFD modeling, *Chem. Eng. R&D* 126 (2017) 19–31.
[14] M. Hosseinzadeh, M. Shirvani, A. Ghaemi, A study on mean drop size and drop size distribution in an eductor liquid-liquid extractor, *Sep. Pur. Technol.* 201 (2018) 205–213.
[15] J. Gu, Q. Xu, H. Zhou, W. Li, J. Zhang, Liquid-liquid mass transfer property of two inline high shear mixers, *Chem. Eng. Process.: Process Intensif.* 101 (2016) 16–24.
[16] C.V. Rajagopalan, K. Periasamy, S.B. Koganti, Development of air pulsed ejector mixer-settlers of different capacities, *In: Proc. Advances in Chemical Engineering in Nuclear and Process Industries (ACE-94))* (1994) 517–523.
[17] H. Sawistowski, Influence of mass-transfer-induced Marangoni effects on magnitude of interfacial area and equipment performance in mass transfer operations, *Chem. Ing. Tech.* 45 (18) (1973) 1114–1117.
[18] D.K. Acharjee, A.K. Mztra, A.N. Roy, Co current flow liquid liquid binary mass transfer in ejectors, *Can. J. Chem. Eng.* 56 (1978) 37–42.
[19] A. Suresh, T.G. Srinivasan, P.R.V. Rao, C.V. Rajagopalan, S.B. Koganti, U/Th separation by counter-current liquid-liquid extraction with tri-sec butyl phosphate by using an ejector mixer-settler, *Separ. Sci. Technol.* 39 (10) (2004) 2477–2496.
[20] H.C. Burkholder, J.C. Berg, Effect of mass transfer on laminar jet breakup: Part I. Liquid jets in gases, *AIChE J.* 20 (5) (1974) 863–872.
[21] S. Kimura, T. Miyauchi, Mass transfer in a liquid—liquid laminar jet, *Chem. Eng. Sci.* 21 (11) (1966) 1057–1065.
[22] H. Cheng, J. Zhao, J. Wang, Experimental investigation on the characteristics of melt jet breakup in water: The importance of surface tension and Rayleigh-Plateau instability, *Ind. Eng. Chem. Res.* 132 (2019) 388–393.
[23] J. Saien, F. Ashrafi, Mass transfer enhancement in liquid– liquid extraction with very dilute aqueous salt solutions, *Ind. Eng. Chem. Res.* 48 (22) (2009) 10008–10014.
[24] A. Tamir, Impinging-stream Reactors: Fundamentals and Applications, Elsevier, 2014.
[25] J. Saien, S. Daliri, Modelling mass transfer coefficient for liquid-liquid extraction with the interface adsorption of hydroxyl ions, *Korean J. Chem. Eng.* 26 (4) (2009) 963–968.
[26] H. Zheng, W. Ren, K. Chen, Y. Gu, Z. Bai, S. Zhao, Influence of Marangoni convection on mass transfer in the *n*-propyl acetate/acetic acid/water system, *Chem. Eng. Sci.* 111 (2014) 278–285.
[27] N. Maan, Mathematical modelling of mass transfer in a multi-stage rotating disc contactor column, Ph.D Thesis, Universiti Teknologi Malaysia, 2006.
[28] M. Asadollahzadeh, A. Hemmati, M. Torab-Mostaedi, M. Shirvani, A. Ghaemi, Z. Mohsenzadeh, Use of axial dispersion model for determination of Sherwood number and mass transfer coefficients in a perforated rotating disc contactor, *Chin. J. Chem. Eng.* 25 (1) (2017) 53–61.
[29] A. Hemmati, M. Shirvani, M. Torab-Mostaedi, A. Ghaemi, Mass transfer coefficients in a perforated rotating disc contactor (PRDC), *Chem. Eng. Process* 100 (2016) 19–25.
[30] L.N. Gomes, M.L. Guimaraes, J. Stichlmair, J.J. Cruz-Pinto, Effects of mass transfer on the steady state and dynamic performance of a kühni column – experimental observations, *Indust. Eng. Chem. Res.* 48 (7) (2009) 3580–3588.
[31] M. Torab-Mostaedi, J. Safdari, A. Ghaemi, Mass transfer coeficients in pulsed perforated-plate extraction columns, *Brazilian J. Chem. Eng.* 27 (2) (2010) 243–251.
[32] M. Asadollahzadeh, A. Ghaemi, M. Torab-Mostaedi, S. Shahhosseini, Experimental mass transfer coefficients in a pilot plant multistage column extractor, *Chin. J. Chem. Eng.* 24 (8) (2016) 989–999.
[33] C. Wilke, P. Chang, Correlation of diffusion coefficients in dilute solutions, *AIChE J.* 1 (2) (1955) 264–270.
[34] A.F. Rusydi, Correlation between conductivity and total dissolved solid in various type of water: A review, *IOP Conf. Ser.: Earth Environ. Sci., IOP Publishing* (2018) 012019.
[35] R.E. Treybal, Mass Transfer Operations, Mcgraw-Hill Book Company Inc., New York, 1980.
[36] A. Nienow, Break-up, coalescence and catastrophic phase inversion in turbulent contactors, *Adv. Colloid Interface Sci.* 108 (2004) 95–103.
[37] W.L. McCabe, J.C. Smith, P. Harriott, Unit Operations of Chemical Engineering, McGraw-hill New York, 1993.
[38] A. Skelland, Y.F. Huang, Dispersed phase mass transfer during drop formation under jetting conditions, *AIChE J.* 23 (5) (1977) 701–714.
[39] A. Skelland, S.S. Minhas, Dispersed phase mass transfer during drop formation and coalescence in liquid-liquid extraction, *AIChE J.* 17 (6) (1971) 1316–1324.
[40] A. Skelland, R. Wellek, Resistance to mass transfer inside droplets, *AIChE J.* 10 (4) (1964) 491–496.
[41] V. Kirou, L.L. Tavlarides, J. Bonnet, C. Tsouris, Flooding, holdup, and drop size measurements in a multistage column extractor, *AIChE J.* 34 (2) (1988) 283–292.
[42] Y. Sun, Q. Zhao, L. Zhang, B. Jiang, Measurement and correlation of the mass-transfer coefficient for the methyl isobutyl ketone-water-phenol system, *Ind. Eng. Chem. Res.* 53 (9) (2014) 3654–3661.
[43] Z. Huang, C. Ye, L. Li, X. Zhang, T. Qiu, Measurement and correlation of the mass transfer coefficient for a liquid-liquid system with high density difference, *Brazilian J. Chem. Eng.* 33 (4) (2016) 897–906.
[44] J. Saien, S.A.E. Zonouzian, A.M. Dehkordi, Investigation of a two impinging-jets contacting device for liquid-liquid extraction processes, *Chem. Eng. Sci.* 61 (12) (2006) 3942–3950.
[45] A. Hemmati, M. Torab-Mostaedi, M. Asadollahzadeh, Mass transfer coefficients in a Kühni extraction column, *Chem. Eng. Process* 93 (2015) 747–754.
[46] M. Wegener, N. Paul, M. Kraume, Fluid dynamics and mass transfer at single droplets in liquid/liquid systems, *Int. J. Heat Mass Transf.* 71 (2014) 475–495.
[47] Y.L. Lee, Surfactants effects on mass transfer during drop-formation and drop falling stages, *AIChE J.* 49 (7) (2003) 1859–1869.
[48] M. Hashem, A. El-Bassuoni, Drop formation mass transfer coefficients in extraction columns, *Theor. Found. Chem. Eng.* 41 (5) (2007) 506–511.
[49] J. Petera, L. Weatherley, Modelling of mass transfer from falling droplets, *Chem. Eng. Sci.* 56 (16) (2001) 4929–4947.
[50] D. Webster, E.K. Longmire, Jet pinch-off and drop formation in immiscible liquid-liquid systems, *Exp. Fluids* 30 (1) (2001) 47–56.
[51] T. Ban, F. Kawaizumi, S. Nii, K. Takahashi, Study of drop coalescence behavior for liquid-liquid extraction operation, *Chem. Eng. Sci.* 55 (22) (2000) 5385–5391.